JOURNAL OF BACTERIOLOGY, Aug. 1992, p. 5414–5423
0021-9193/92/165414-10$02.00/0

Vol. 174, No. 16

Isolation and Characterization of *ftsZ* Alleles That Affect Septal Morphology

ERFEI BI† AND JOE LUTKENHAUS*

Department of Microbiology, Molecular Genetics, and Immunology, University of Kansas Medical Center, Kansas City, Kansas 66103

Received 10 March 1992/Accepted 11 June 1992

The *ftsZ* gene encodes an essential cell division protein that specifically localizes to the septum of dividing cells. In this study we characterized the effects of the *ftsZ2*(Rsa) mutation on cell physiology. We found that this mutation caused an altered cell morphology that included minicell formation and an increased average cell length. In addition, this mutation caused a temperature-dependent effect on cell lysis. During this investigation we fortuitously isolated a novel temperature-sensitive *ftsZ* mutation that consisted of a 6-codon insertion near the 5′ end of the gene. This mutation, designated *ftsZ26*(Ts), caused an altered polar morphology at the permissive temperature and blocked cell division at the nonpermissive temperature. The altered polar morphology resulted from cell division and correlated with an altered geometry of the FtsZ ring. An intragenic cold-sensitive suppressor of *ftsZ26*(Ts) that caused cell lysis at the nonpermissive temperature was isolated. These results support the hypothesis that the FtsZ ring determines the division site and interacts with the septal biosynthetic machinery.

The *ftsZ* gene was classified as a cell division gene on the basis of the filamentous phenotype conferred by the conditional lethal *ftsZ84*(Ts) mutation at the nonpermissive temperature (16). More recently this designation was confirmed when it was shown that the *ftsZ* gene was essential and that reducing expression of the gene led to inhibition of division (6, 18, 24). Surprisingly, however, the *ftsZ84*(Ts) mutation remains the only conditional lethal mutation in the *ftsZ* gene, as no additional alleles were found among cell division mutants selected on the basis of a filamenting phenotype (9). In contrast, numerous conditional lethal mutations have been found in the *ftsA* and *ftsI* genes.

In the absence of *ftsZ* function, observed in strains that conditionally express *ftsZ* or express the *ftsZ84*(Ts) mutation, cells form smooth filaments with no sign of constriction (6). Such morphology suggests that FtsZ acts earlier in cell division than other known *fts* genes, since mutations in these genes result in filaments with indentations at regular intervals that may be aborted or stalled division attempts (9). In contrast to the effect of reducing *ftsZ* expression, slight overexpression of *ftsZ* results in hyperdivision activity in the form of a minicell phenotype, although further overexpression also inhibits division (1, 25). Such studies have suggested that FtsZ is rate limiting for division.

Recent localization of FtsZ by using immunoelectron microscopy revealed that FtsZ is located at the leading edge of the septal invagination (4). The results demonstrated that FtsZ assembles at the midpoint of the cell in a ringlike structure prior to septation. This FtsZ ring is present throughout septation but disassembles upon completion of septation. It was suggested that the FtsZ ring forms a cytoskeletal element that determines the division site and activates the division process.

A class of mutations, selected on the basis of resistance to the cell division inhibitor, SulA, map in the *ftsZ* gene and have been designated *ftsZ*(Rsa) (2). These mutations appear to alter the *ftsZ* gene product such that it is resistant to SulA (14, 15). These same mutations also confer increased resistance to the cell division inhibitor MinCD, which is part of the *min* system (3). Although these mutations are not conditional lethals, at least some of these *ftsZ*(Rsa) mutations confer a slightly temperature-sensitive cell division phenotype, especially at low salt concentrations (10, 12, 13). Most of these *ftsZ*(Rsa) mutations were isolated at the chromosomal locus; however, *ftsZ1*(Rsa), *ftsZ2*(Rsa), and *ftsZ3* (Rsa) were obtained on a low-copy vector in the presence of a wild-type allele on the chromosome (2). Of these alleles it was demonstrated that *ftsZ3*(Rsa) conferred resistance to SulA and MinCD in the presence of *ftsZ* but could not substitute for *ftsZ* for cell viability. Further examination of the properties of *ftsZ3*(Rsa) indicated that FtsZ must function as a multimer.

In this paper we further characterize the *ftsZ2*(Rsa) mutation, and during this process we isolated additional conditional lethal mutations in the *ftsZ* gene. Each of these mutations has dramatic effects on cell physiology, including altered septal morphology, minicell formation, and cell lysis.

MATERIALS AND METHODS

Bacterial strains, phages, and plasmids. The strains used are all derivatives of MC4100 and W3110 and are listed in Table 1. Phage λ 16-2 (*imm*^{21}) is a transducing phage carrying a 10-kb chromosomal insert including the *ftsZ* gene (16). λ BEF2 is identical to λ 16-2 except that it carries the *ftsZ2*(Rsa) mutation (2). λDB173 carries the *minCD* genes downstream of the *lac* promoter and has been described elsewhere (8). pKD3 contains the *ftsA*, *ftsZ*, *envA*, and gene *X* genes on a *Bam*HI fragment in the temperature-sensitive pSC101 derivative pEL3 (6). pBEF0 contains the same *Bam*HI fragment in pGB2, also a derivative of pSC101 (1). pBEF2 is identical to pBEF0 except that it contains *ftsZ2*(Rsa) (2). pBEF20 contains the *recA* gene cloned into a pBR322 derivative that is Kan^r. pELEZ2 contains the 5′ truncated *ftsZ* gene on an *Eco*RI fragment cloned into pEL3.

* Corresponding author.
† Present address: Department of Biology, University of North Carolina, Chapel Hill, NC 27599.

TABLE 1. Bacterial strains

Strain	Relevant marker	Source or reference
MC4100		4
W3110		Laboratory collection
JKD7-1(pKD3)	*ftsZ*::*kan recA56 srl*::Tn*10*	6
JKD7-3(λ 16-2)	ftsZ::*kan recA56 srl*::Tn*10*	6
JKD7-3(λ BEF2)	ftsZ::*kan recA56 srl*::Tn*10*	6
JKD26(λ BEF2)	ftsZ26(Ts) *recA56 srl*::Tn*10*	This study
JKD26(pKD3)	ftsZ26(Ts) *recA56 srl*::Tn*10*	This study
MC26	As MC4100, but *leu*::Tn*10 ftsZ26*(Ts)	This study
MCS261	As MC26, but also *ftsZ261*(Cs)	This study
JFL101	ftsZ84(Ts) *recA*	16

The *Eco*RI fragment containing most of the *ftsZ* gene and the *envA* gene was obtained from pBEF2.

Media and growth conditions. The media used throughout these experiments was L broth supplemented with thymine (50 μg/ml) and the appropriate antibiotics. Antibiotics were used at the following concentrations: ampicillin, 100 μg/ml; tetracycline, 12.5 μg/ml; chloramphenicol, 17 μg/ml; and spectinomycin, 25 μg/ml.

Genetic manipulations. To determine if suppressor mutations of *ftsZ2*(Rsa) that were obtained in JKD7-3(λBEF2) were on the prophage or the bacterial chromosome, the prophage was replaced with fresh λ BEF2. Strains carrying the suppressor mutations were transformed with pKD3 and cured of the resident λ BEF2 by using λ*b*2. Curing of λ lysogens that carry immunity to phage 21 was done by spotting a dilution of the heteroimmune phage λ*b*2 (*imm*$^{\lambda}$) on a lawn of the lysogen. Survivors isolated from the plaque were tested to determine if they had been cured. Cured strains were then lysogenized with fresh λ BEF2 and grown at 37°C to cure the plasmid. One of these suppressor mutations, present in JKD26, was subsequently shown to contain a mutation in *ftsZ*, which was designated the *ftsZ26*(Ts) mutation. The *ftsZ26*(Ts) mutation was introduced into the MC4100 background as described below. JKD26 was cured of Tn*10* to obtain a derivative that was Tet^{s} (7). This derivative was then transformed with pBEF20 to make the strain *recA*$^{+}$ for doing transductions. P1 grown on NK6923 (*leu*::Tn*10*) was used to transduce the *recA*$^{+}$ derivative to Tet^{r}. One of these transductants that was still temperature sensitive was used as a donor for transduction of *leu*::Tn*10* into MC4100. One of the Tet^{r} transductants that had become temperature sensitive was designated MC26.

Nitrosoguanidine mutagenesis. Nitrosoguanidine mutagenesis was essentially done as described by Miller (17). Revertants of MC26 [*ftsZ26*(Ts)] were isolated after nitrosoguanidine treatment that resulted in 50% killing. Among 498 temperature-resistant colonies, 13 were found to be cold sensitive.

Photomicroscopy. Cells were fixed in the growth medium with 2% glutaraldehyde and photographed with a light microscope or a scanning electron microscope. Nucleoid staining with 4′,6-diamidino-2-phenylindole was done essentially as described by Hiraga et al. (11).

DNA sequencing. Dideoxy sequencing was performed as previously described (2).

Immunoelectron microscopy. Cells were processed for immunoelectron microscopy as previously described (4).

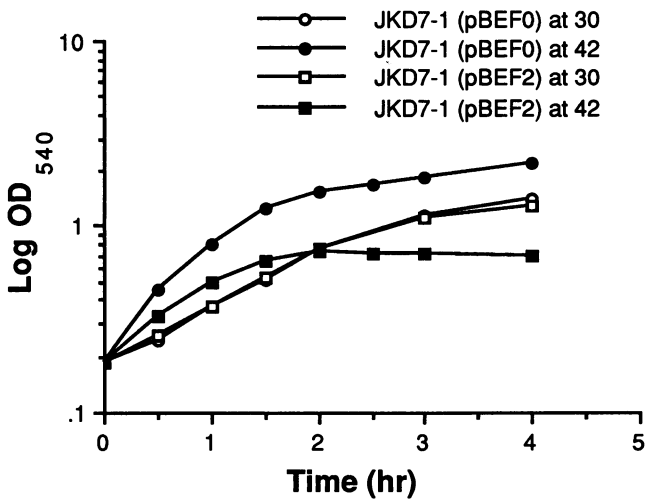

FIG. 1. Effects of the *ftsZ2*(Rsa) mutation on cell growth. Exponentially growing cultures of JKD7-1(pBEF2) and JKD7-1(pBEF0) at 30°C were inoculated at 30 and 42°C at time zero.

RESULTS

Characterization of *ftsZ2*(Rsa). To determine the effect of the *ftsZ2*(Rsa) mutation on *ftsZ* function, a plasmid carrying *ftsZ2*(Rsa), pBEF2, was introduced into JFL101 [*ftsZ84*(Ts) *recA*]). As controls, the plasmids pBEF0 (*ftsZ*$^{+}$) and pGB2 (parent vector) were used. Whereas plasmid pBEF0 complemented *ftsZ84*(Ts) at 42°C on plates, pBEF2 and pGB2 did not. After a shift to nonpermissive temperature in liquid culture JFL101 containing pGB2 continued to increase in optical density for several generations with the formation of long filaments, whereas the presence of pBEF0 completely suppressed filament formation. In contrast, JFL101 containing pBEF2 showed only a small increase in optical density after a shift to the nonpermissive temperature. Microscopic examination of this latter culture revealed some cell lysis at the permissive temperature which was dramatically increased at the nonpermissive temperature. The presence of pBEF2 also affected cell morphology even at the permissive temperature. Cells were heterogeneous in length and had malformed ends often associated with minicells, characteristics that were not affected by temperature.

Since FtsZ is thought to function as a multimer (2), the phenotypes associated with *ftsZ2*(Rsa) may be influenced by the presence of the *ftsZ84*(Ts) allele. To eliminate this possibility, pBEF2 was introduced into JKD7-1(pKD3). This strain contains an interrupted *ftsZ* allele (*ftsZ*::*kan*) on the chromosome and a plasmid that is temperature sensitive for replication and contains *ftsZ* (6). Since these two plasmids are not compatible, selection for pBEF2 should displace pKD3, provided the *ftsZ2*(Rsa) allele can support cell growth. Selection for Spc^{r} resulted in the loss of Amp^{r}, indicating that *ftsZ2*(Rsa) on a low-copy vector could support cell growth. Any phenotypic differences between this strain, JKD7-1(pBEF2), and the wild-type control, JKD7-1(pBEF0), can be attributed to the *ftsZ2*(Rsa) mutation.

As seen in Fig. 1, the growth curve for JKD7-1(pBEF2) was superimposable with the control strain at 30°C, whereas at 42°C the cell mass increased for only a short time before ceasing. Microscopic examination of the cultures revealed that the presence of pBEF2 in this strain resulted in cells with a heterogeneous cell length distribution and a significant

minicell phenotype at both temperatures (Fig. 2 [only the 30°C cultures are shown]). This phenotype is similar to the phenotype induced by mutations at the *min* locus, which also results in septation occurring at the cell poles and a longer average cell length for nucleoid-containing cells (21). A distinguishing characteristic of the phenotype resulting from pBEF2 was the altered polar morphology, especially very blunt poles often associated with minicells that were of variable size and not always spherical. At 30°C some cell lysis was observed with pBEF2, but this increased significantly at 42°C. Also, the average cell length did not increase at 42°C, indicating that cell division was continuing as long as the mass continued to increase. Examination of nucleoid segregation revealed that segregation was normal in the elongated cells that are present at 30°C (Fig. 3).

The readily observable minicell phenotype seen with pBEF2 contrasts with the barely detectable minicell phenotype induced by pBEF0. This phenotype is expected with pBEF0, which compensates for the disrupted chromosomal locus and provides approximately the wild-type level of FtsZ. Immunoblot analysis revealed that each plasmid led to the same level of FtsZ (data not shown), suggesting that FtsZ2 can ignore the topological specificity normally imposed by the *min* system and initiate division at the poles (8).

We previously showed that *ftsZ2*(Rsa) could protect against overexpression of *minCD* in the presence of a wild-type copy of the *ftsZ* gene (3). To determine if *ftsZ2*(Rsa) could provide resistance to MinCD in the absence of the wild-type gene, JKD7-1(pBEF2) was lysogenized with λ DB173. Induction of *minCD* in the presence of pBEF2 had no effect on cell morphology, whereas induction in the presence of pBEF0 resulted in filamentation (data not shown). These results confirmed that *ftsZ2*(Rsa) was resistant to *minCD*.

The best situation for studying the physiological effects of *ftsZ2*(Rsa) would be to introduce this allele at the normal chromosomal locus since this would ensure that the regulation was normal. Introduction of pBEF2 into JKD7-1(pKD3) and displacement of pKD3 demonstrated that *ftsZ2*(Rsa) could support cell growth. Therefore, pELEZ2, which confers Amp^r and carries a fragment containing the 5′ truncated *ftsZ2*(Rsa) allele and the downstream *envA* gene, was transfected into a strain carrying *leu*::Tn*10*. Plating at 42°C, which is nonpermissive for plasmid replication, in the presence of ampicillin selects for cells in which the plasmid has integrated. Subsequent incubation of such integrants at 30°C should lead to resolution and loss of the plasmid. Two colonies from ampicillin plates at 42°C were grown overnight at 30°C in the presence of ampicillin and then diluted and grown overnight in the presence of tetracycline without ampicillin. The cultures were plated onto tetracycline plates and replica plated to ampicillin plates, all at 30°C. Ninety percent of the colonies were Amp^s, indicating loss of the plasmid. Of a total of 149 Amp^s colonies obtained from the two integrants, none were found to be temperature sensitive. We would have expected that approximately 25% of these colonies should have retained the *ftsZ2*(Rsa) allele and become temperature sensitive (on the basis of the relative lengths of the flanking sequences). We also expected that retention of the *ftsZ2*(Rsa) allele would have affected cell morphology, especially at the cell poles. A total of 24 colonies were screened microscopically, but only wild-type morphology was observed. These results suggest that *ftsZ2*(Rsa) cannot support cell growth when present at the normal locus. These results suggest that the FtsZ2 protein is less active than the wild type, but this reduced activity can be compensated for by an increased gene dosage to support cell growth.

The transducing phage λ 16-2 introduced at the *att* locus does not produce as much FtsZ as the chromosomal *ftsZ* locus and cannot complement the interrupted *ftsZ* allele present in JKD7-1 (6). JKD7-3 is a derivative of JKD7-1 that contains an uncharacterized chromosomal mutation that allows λ 16-2 to complement the null allele (6). We were able to replace λ 16-2 in JKD7-3 with λ BEF2 as outlined in Materials and Methods. The resultant strain grew best at 37°C, although even at this temperature growth was slow compared with that of the control strain. The morphology of this lysogen was very similar to that of JKD7-1(pBEF2) with lysed cells and minicells observed at all temperatures, but cell lysis enhanced at 42°C. On plates at 30°C faster growing colonies arose at a high frequency. Since these colonies could carry extragenic suppressors of *ftsZ2*(Rsa), they were further investigated.

Isolation of a new *ftsZ*(Ts) mutation. Faster-growing colonies of JKD7-3(λ BEF2) could be divided into two classes on the basis of morphology. The first class had several aspects of the original mutant morphology, including minicell formation and a heterogeneous cell length distribution, but the cell lysis phenotype was completely absent. The second class of suppressor still produced minicells, but other morphological aspects of the *ftsZ2*(Rsa) mutation were suppressed. One mutant from each class was chosen, and it was determined that in both cases the suppressor mutation was on the chromosome and not the phage. This was done by curing the resident λ BEF2 and replacing it with a fresh λ BEF2 (as described in Materials and Methods) and finding that the *ftsZ2*(Rsa) mutation was still suppressed. Since the second class of suppressors provided more complete suppression of the morphological aspects of the *ftsZ2*(Rsa) phenotype, it was studied further.

Microscopic examination of JKD26, which contained one of the suppressing mutations, grown at different temperatures revealed that the suppression was temperature sensitive. At 30 and 37°C the morphological aspects of the *ftsZ2*(Rsa) phenotypes were suppressed, but at 42°C they were not. Subsequently, we determined that JKD26 was Kan^s. We had not used kanamycin during the selection, thinking that the *ftsZ*::*kan* allele was quite stable in a *recA* background. Deletion of the *kan* element could restore *ftsZ* function and therefore suppress *ftsZ2*(Rsa). If this occurred it could not have been a precise excision, since the suppressor function was temperature sensitive. Precise excision would have resulted in an intact *ftsZ* gene and complementation of *ftsZ2*(Rsa). Since the *kan* element is flanked by moderate-length inverted repeats that contain an internal short direct repeat (8 bp including the *Bam*HI site [Fig. 4]), excision somewhere within the repeat could generate an *ftsZ* allele with a small insertion depending upon where the crossover occurred. To determine if this was the case, this *ftsZ* allele, designated *ftsZ26*(Ts), was cloned and analyzed by restriction enzyme analysis. The presence of *Eco*RI and *Bam*HI sites but lack of a *Sal*I site indicated that excision of the *kan* element had occurred, leaving behind at least some DNA. The absence of a *Bspe*I site along with the above information was diagnostic that 6 codons were left behind by the excision event (Fig. 4).

To determine if the *ftsZ26*(Ts) allele could support cell growth and to determine its effects on cell physiology, JKD26 was cured of λ BEF2. Since λ BEF2 could be easily cured at 30°C, it demonstrated that the *ftsZ26*(Ts) allele could support cell growth. For a more careful examination of

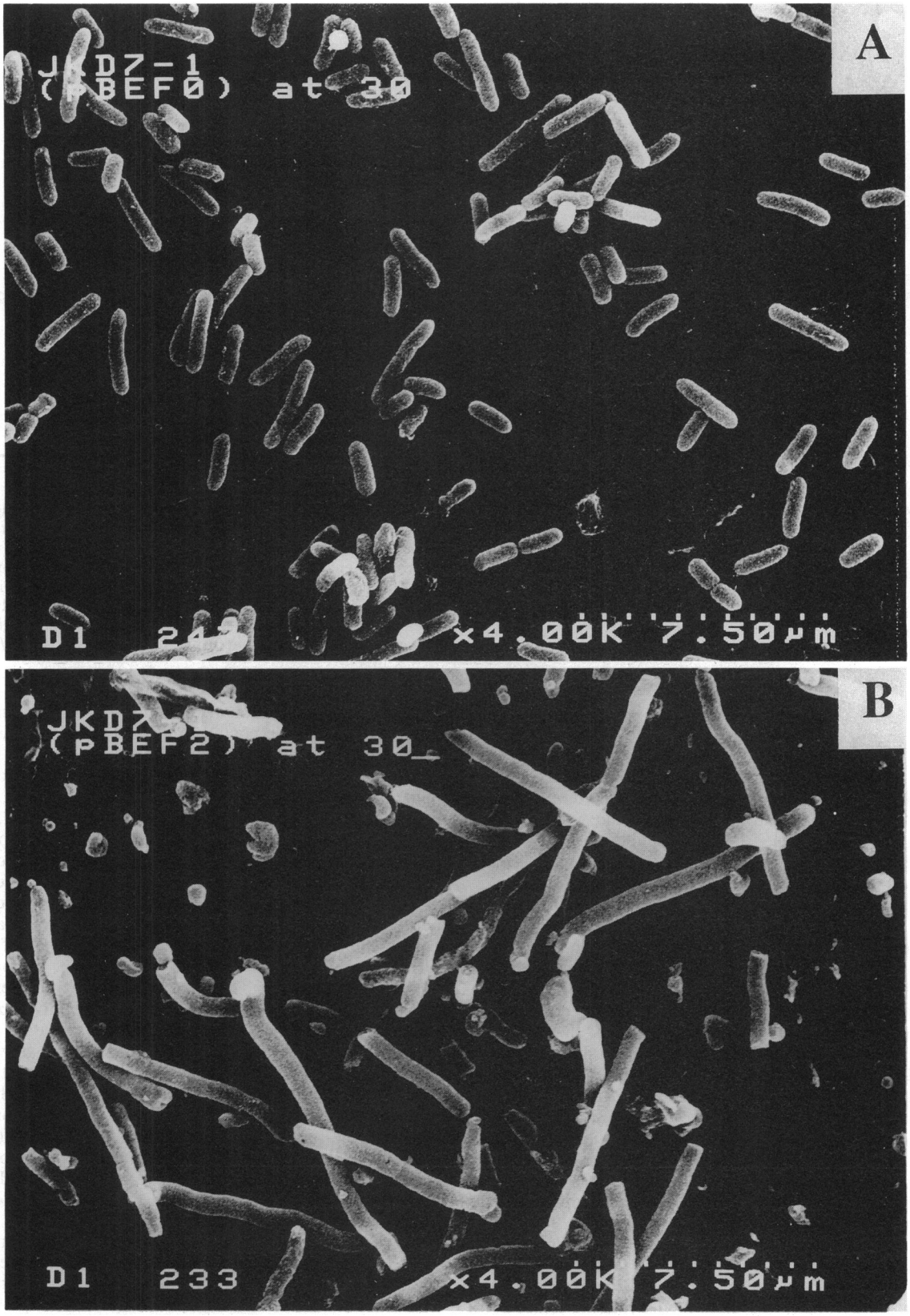

FIG. 2. Effects of the *ftsZ2*(Rsa) mutation on cell morphology. Samples of exponential cultures growing at 30°C of JKD7-1(pBEF0) (A) and JKD7-1(pBEF2) (B) were processed for scanning electron microscopy. Magnification, ×4,000.

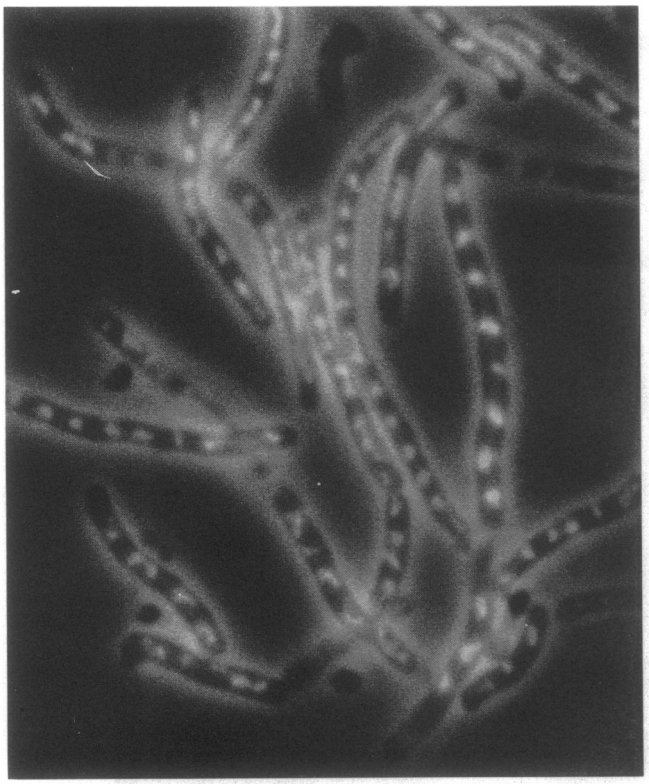

FIG. 3. Effects of the *ftsZ2*(Rsa) mutation on DNA segregation. An exponentially growing culture of JKD7-1(pBEF2) was stained with 4′,6-diamidino-2-phenylindole to examine nucleoid segregation at 30°C.

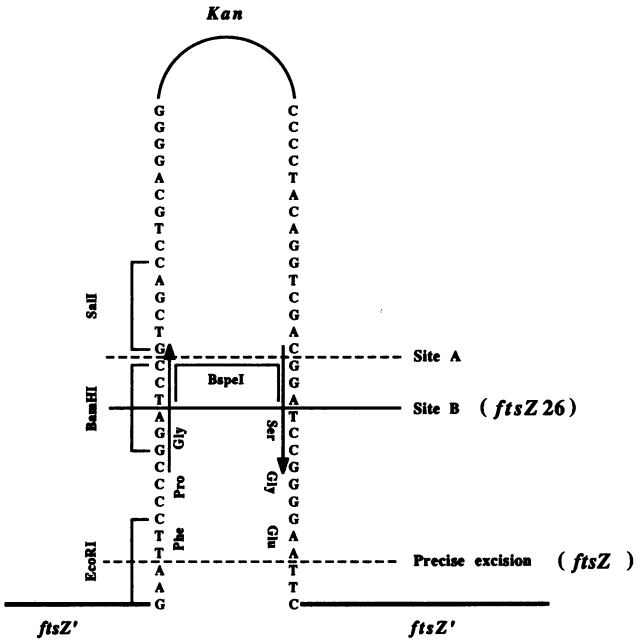

FIG. 4. Diagram indicating the deletion event giving rise to *ftsZ26*(Ts). The nucleotide sequence of the inverted repeats flanking the *kan* element inserted at the *Eco*RI site in the *ftsZ* gene is shown. Restriction enzyme analysis which was subsequently confirmed by DNA sequencing demonstrated that the deletion event giving rise to *ftsZ26*(Ts) occurred at site B. The *ftsZ26*(Ts) allele has 18 nucleotides inserted at the *Eco*RI site coding for 6 additional amino acids. Precise excision would have resulted in restoration of the *ftsZ* gene.

the effects of the *ftsZ26*(Ts) mutation, it was transduced to MC4100 (as described in Materials and Methods). The transductant, MC26, grew at 30°C but was temperature sensitive for colony formation. Microscopic examination revealed that cell morphology was affected by the *ftsZ26*(Ts) mutation even at 30°C (Fig. 5A). The most noticeable effect was an altered morphology of the cell ends, which included minicell formation. Although some poles appeared normal, with rounded hemispherical morphology, many cells had poles which were blunt and had protrusions to one side. These protrusions appeared to arise from the cell division process, as dividing cells that were not aligned along a central axis were often observed. In addition, cells were more elongated than the wild type, and some Y-shaped cells were observed. After a shift to the nonpermissive temperature, MC26 formed filaments that were similar in morphology to filaments formed from expression of the *ftsZ84*(Ts) mutation except for the poles which are formed at 30°C (Fig. 5B). Nucleoids were evenly distributed in the *ftsZ26* filaments, as has been reported for *ftsZ84* filaments (data not shown). In addition, the *ftsZ26*(Ts) mutation was recessive, as the temperature sensitivity was completely suppressed by λ 16-2.

To examine cell division more closely in MC26 and to determine the effect of the *ftsZ26*(Ts) mutation on the formation of the FtsZ ring, a sample of MC26 growing at the permissive temperature was examined by immunoelectron microscopy. Figure 6 shows examples of dividing cells that were prevalent in the population. Cells displaying normal division morphology were also observed. In the cells shown in Fig. 6 the division constriction has an abnormal morphology that would be expected to lead to cells with misshapen poles. The position of FtsZ is indicated by the gold particles which appear as dark spots in the photograph. The primary defect appears to be that the FtsZ ring(s) present in these cells is not perpendicular to the long axis of the cell, as seen in wild-type cells. In one of the cells the FtsZ is located at the apexes of a triangle. This localization would be consistent with two FtsZ rings that are adjacent on one side of the cell but each veering off at an angle such that neither ring is perpendicular to the long axis of the cell. This pattern of FtsZ localization could also explain the low level of minicell formation seen with the *ftsZ26*(Ts) mutation. In contrast to *ftsZ2*(Rsa), the *ftsZ26*(Ts) mutation does not suppress *lon* or the filamentation caused by expression of MinCD expressed from the *lac* promoter, indicating that this mutation does not confer resistance to SulA or MinCD (data not shown). This suggests that FtsZ26 would not be able to ignore the topological specificity imposed by *min* and act directly at the poles, as suggested for FtsZ2. Instead, the electron micrographs show that minicell formation due to *ftsZ26*(Ts) mutation probably occurs through formation of two closely spaced FtsZ rings at the cell center. Division mediated by each of these closely positioned rings would lead to the formation of a minicell in the center of the cell.

Isolation of a cold-sensitive allele of *ftsZ*. To determine if an extragenic suppressor of *ftsZ26*(Ts) could be isolated, strain MC26 was mutagenized (as described in Materials and Methods) and survivors selected at 42°C. Among 498 survivors at 42°C, 13 were found to be cold sensitive for growth at 30°C. Of these 13, 4 were chosen for further study since they showed the most cold-temperature sensitivity. P1 transduc-

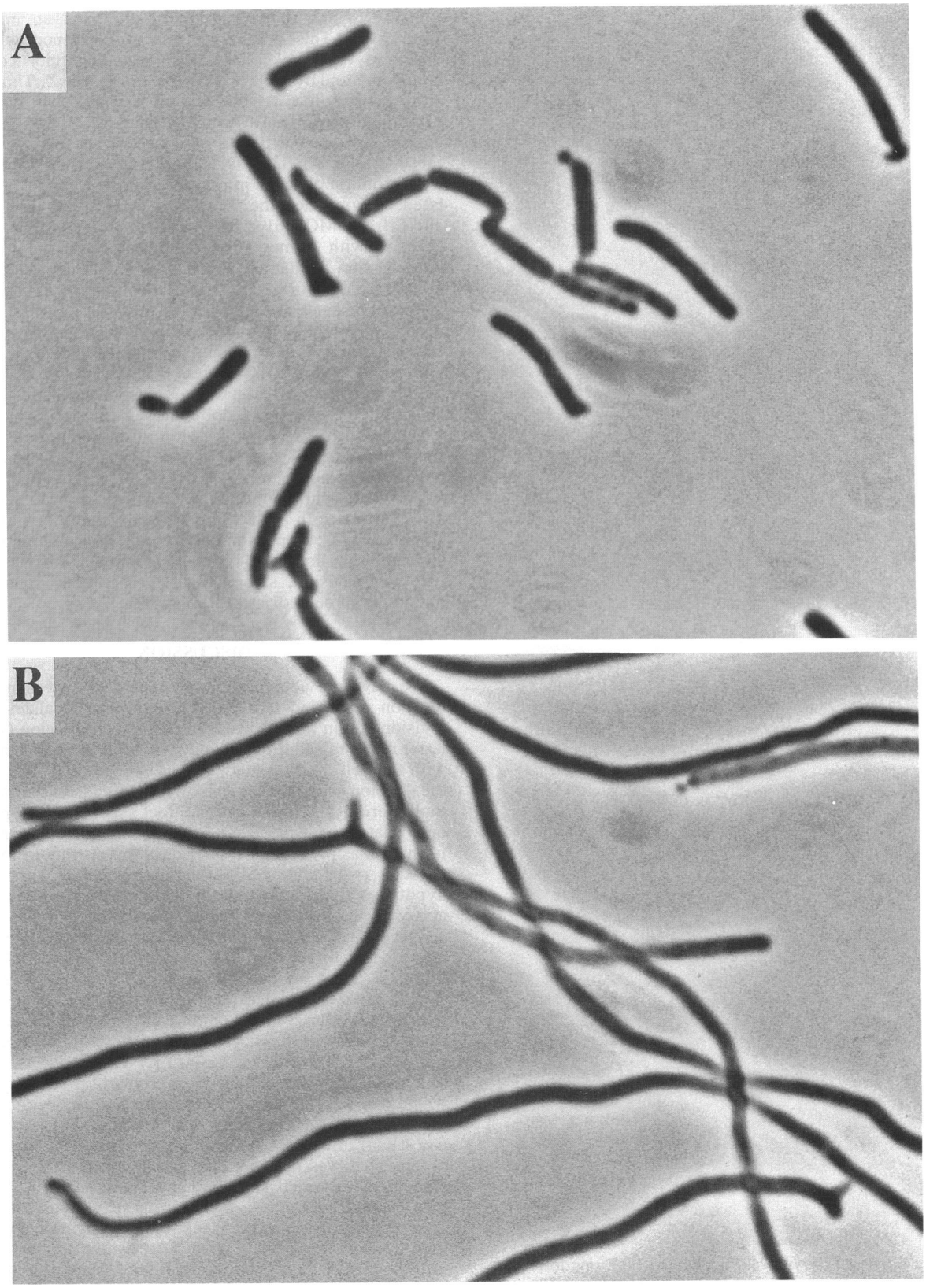

FIG. 5. Effects of the *ftsZ26*(Ts) allele on cell division. An exponential culture of MC26 [*ftsZ26*(Ts)] was photographed at 30°C (A) or 2 h after a shift to 42°C (B).

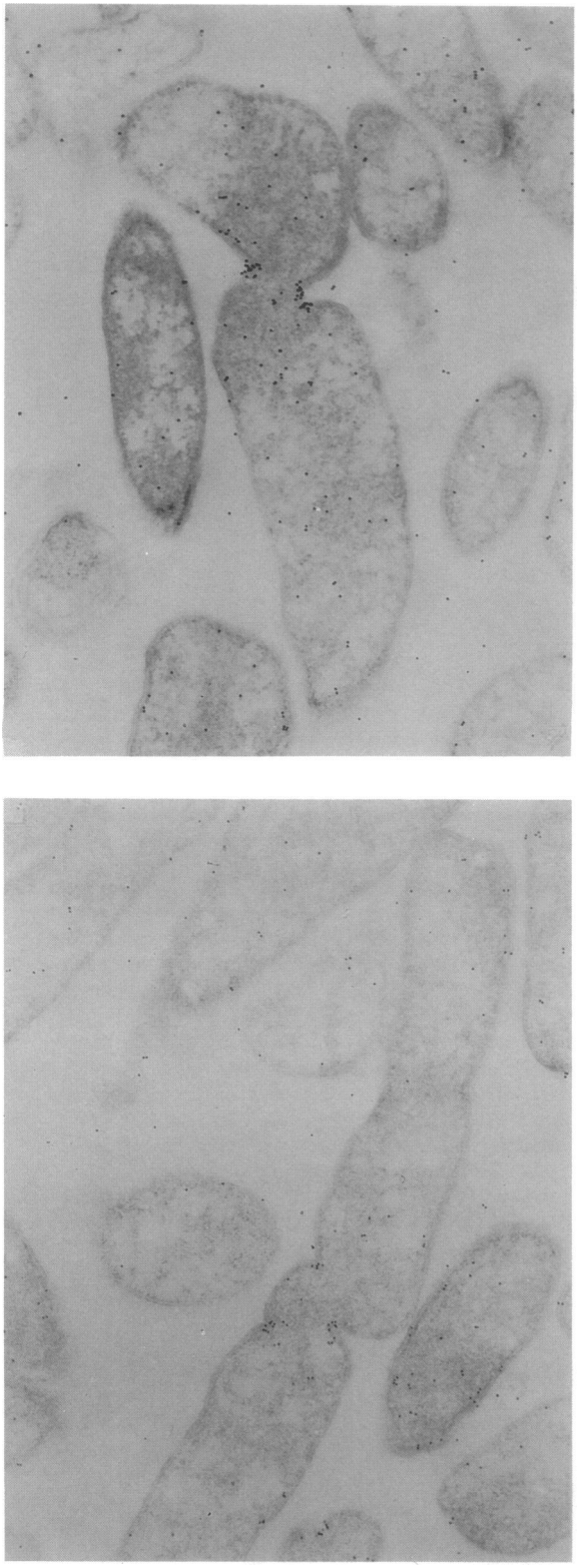

FIG. 6. Effects of the *ftsZ26*(Ts) allele on FtsZ ring formation. An exponential culture of MC26 [*ftsZ26*(Ts)] growing at 30°C was processed for immunoelectron microscopy, and the location of FtsZ26 was determined by indirect immunogold labelling.

tion data showed that the cold-sensitive mutation was linked to *ftsZ*, raising the possibility that it was an intragenic suppressor. This possibility was strengthened when we observed that the cold-temperature sensitivity could be complemented by pKD4, which carries just *ftsZ*. Thus, these strains appear to carry two mutations in *ftsZ*, one consisting of a 6-codon insertion at the *Eco*RI site near the 5′ end of the gene and a second giving rise to cold sensitivity. One of these strains, MCS261, was chosen for further study.

To confirm that an intragenic suppressor had been isolated, we obtained the *ftsZ* allele from MCS261. The *ftsZ* allele from MCS261 was obtained by polymerase chain reaction with primers that did not include the ribosome binding site. Sequence analysis of this allele, designated *ftsZ261*(Cs), confirmed the presence of the 6-codon insertion at the *Eco*RI site [the *ftsZ26*(Ts) mutation] and revealed a nearby single-point mutation. The alteration was a C-to-T transition at codon 11 resulting in replacement of alanine with valine. This point mutation alone or in combination with the *ftsZ26*(Ts) mutation is responsible for the cold sensitivity, as they have not been separated.

Depletion of *ftsZ* or expression of the temperature-sensitive phenotypes of *ftsZ84*(Ts) or *ftsZ26*(Ts) leads to filamentation (5, 6; this study). To determine the effect of the *ftsZ261*(Cs) mutation on cell morphology, MCS261 was grown in L broth at 42°C for several generations and then shifted to 30°C. Approximately 30 min after the temperature shift, the cells started to lyse. Lysis appears to be associated with cell division, since bulges were mostly seen at the midpoints of cells or at cell poles (Fig. 7).

DISCUSSION

We have previously shown that *ftsZ* is an essential cell division gene and that the FtsZ protein localizes to the division site in a ring structure during cell division (4). This latter result raised the possibility that the FtsZ ring interacts with the cell division machinery to coordinate and activate the division process. The results presented here demonstrate that altering *ftsZ* function can affect aspects of cell physiology related to cell division, including not only minicell formation as previously reported (2) but also morphology of the cell poles and cell lysis. These results support the hypothesis that FtsZ determines the division site and interacts with the septal biosynthetic machinery.

The present study involved the analysis of the phenotypes induced by three new *ftsZ* alleles, each of which has a dramatic effect on cell division. The first one examined, *ftsZ2*(Rsa), was isolated recently by selecting for resistance to SulA (2). Our results demonstrate that this allele cannot support cell growth when placed at the chromosomal location but can if placed on a plasmid. This suggests that the *ftsZ2*(Rsa) mutation reduces the activity of the FtsZ protein, which can be compensated for by increasing the amount of the gene product to support cell survival. The presence of *ftsZ2*(Rsa) affected cell physiology in several ways. Most pronounced was the effect on cell division, which included elongated nucleated cells with normally segregated nucleoids and the production of minicells of various diameters. This phenotype is similar to that of a *min* mutant (8, 22) and may be explained by the MinCD-resistant phenotype conferred by *ftsZ2*(Rsa). Another feature of the morphology was the abnormal cell ends, which included blunt ends and ends that were otherwise distorted. This altered morphology is also due in part to the MinCD-resistant feature of *ftsZ2*(Rsa) which gives it access to the poles, and, in addition, we

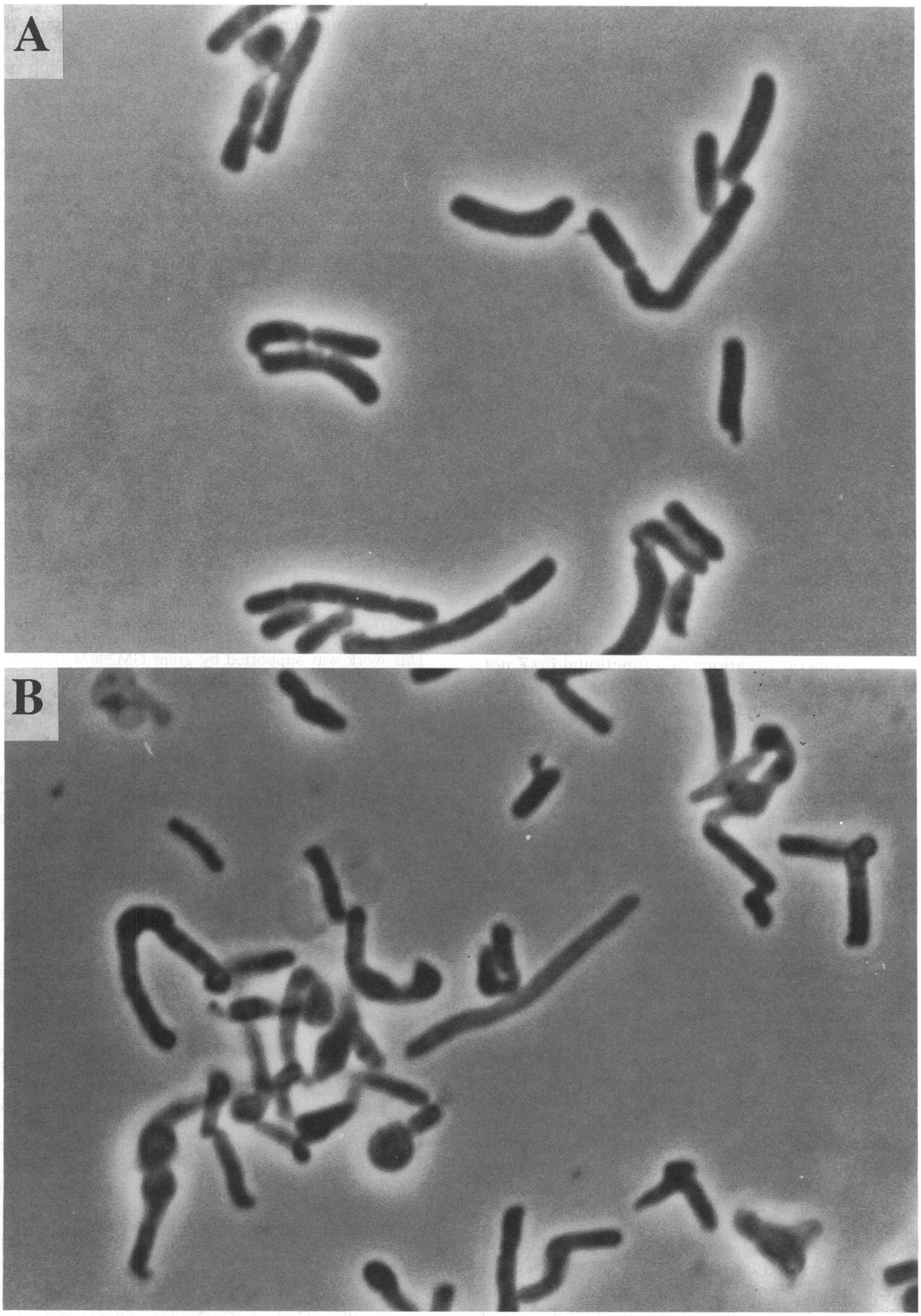

FIG. 7. The *ftsZ261*(Cs) mutation causes cell lysis. An exponentially growing culture of MC261 [*ftsZ261*(Cs)] was photographed after growth at 42°C (A) or 2 h after a shift to 30°C (B).

propose that it is due to an altered FtsZ ring assembly or an altered interaction of the FtsZ ring and the septal biosynthetic machinery. Either of these latter possibilities could give the altered septal morphology, the variable minicell size, and perhaps also the cell lysis. This latter aspect of the cell morphology is temperature dependent. Since division continues at the nonpermissive temperature, we assume that the FtsZ ring continues to assemble at the high temperature but its function is altered, leading to cell lysis. We suspect that the lysis is due to poor coordination between the FtsZ ring and the septal biosynthetic machinery.

The *ftsZ26*(Ts) mutation was isolated fortuitously as a result of deletion of the *kan* element present in the *ftsZ::kan* allele. Although the *kan* element is flanked by large inverted repeats, the deletion could have been mediated by the short direct repeats contained within the inverted repeats (19). The *ftsZ26*(Ts) mutation results in a temperature-sensitive filamentous phenotype that resembles that caused by the *ftsZ84*(Ts) mutation. At the nonpermissive temperature both mutations result in the formation of smooth filaments characteristic of lack of *ftsZ* function. However, at the permissive temperature there is a dramatic difference in cell morphology. Whereas *ftsZ84* mutant cells appear like the wild type, the *ftsZ26* mutant cells have a very high frequency of altered polar morphology. This morphology can be best summarized as abnormally shaped cell poles that are produced during the cell division process. Since the filaments produced by *ftsZ26*(Ts) at the nonpermissive temperature appear normal (except for the altered poles already present at 30°C), cell elongation must be normal. This is consistent with FtsZ26 not functioning at the nonpermissive temperature and with previous observations of a functional FtsZ not being required for cell elongation (6). At the permissive temperature the altered cell poles must arise from the altered action of FtsZ26 during the division process. The immunoelectron microscopy demonstrated that the rings formed by the FtsZ26 protein were not perpendicular to the long axis of the cell but were skewed. We believe that it is this altered geometry of the FtsZ ring that leads to the altered polar morphology in the *ftsZ26* mutant and most likely to the blunt polar morphology observed with the *ftsZ2*(Rsa) mutant as well. In addition, the altered geometry of the FtsZ ring observed in the *ftsZ26* mutant suggests that the structure of the ring is an intrinsic property of the FtsZ protein. This is consistent with the proposal that the FtsZ ring is formed through self-assembly of FtsZ subunits. It is intriguing that with FtsZ26 two rings that are closely positioned are occasionally formed (Fig. 6). We believe that this is due to an altered self-assembly property of the mutant protein.

Another aspect of the involvement of FtsZ in cell division is revealed by the *ftsZ26*(Ts), *ftsZ2*(Rsa), and *ftsZ261*(Cs) mutations. These latter two mutations both lead to cell lysis at the nonpermissive temperature. Whereas the mechanism of lysis caused by *ftsZ2*(Rsa) is not suggested by examining the cell morphology, a mechanism for the lysis caused by *ftsZ261*(Cs) is suggested by the cell morphology. In this latter case the lysis results from bulges that arise at midcell or at the cell poles, suggesting that it is coupled to cell division. This morphology suggests that *ftsZ261*(Cs) exacerbates the phenotype caused by *ftsZ26*(Ts) at 30°C. Whereas *ftsZ26*(Ts) leads to abnormal polar morphology, the *ftsZ261*(Cs) mutation results in a more severe phenotype that includes lysis. We suspect that the lysis is due to this mutationally altered FtsZ protein forming division rings at 30°C which initiate septation but no longer effectively coordinate the septation machinery which results in cell lysis with *ftsZ261*(Cs).

What components of the septal biosynthetic machinery might FtsZ interact with? It is likely that FtsZ must interact with penicillin-binding protein 3 (PBP3), which is uniquely required for division (20). It has been suggested that PBP3 may interact with FtsA (23) and it is possible that FtsZ may influence PBP3 activity directly or indirectly through FtsA or some other protein. It has been reported that amino acid substitutions in PBP3 affect polar morphology (21). In this case the altered polar morphology consists of cells with pointed ends and appears to be due to reduced PBP3 activity. This is consistent with PBP3 being the primary peptidoglycan-synthesizing enzyme during septation and a reduced activity of this enzyme slowing down the septation process leading to the pointed poles instead of rounded hemispherical poles. We hypothesized that the FtsZ ring provides a cytoskeletal element that leads to a localized activation of PBP3 and thereby influences septal biosynthesis. A decrease in PBP3 activity, but insufficient to block division, may hamper the dynamics of the FtsZ ring such that the shape of the poles becomes pointed. With the *ftsZ* mutants described here the effect on polar morphology is a direct result of the altered geometry of the FtsZ ring, and in the instances where lysis occurs we believe it is due to a decrease in coordination between the mutant FtsZ ring and the septal biosynthetic machinery. It is clear from the results presented here that it is the geometry of the FtsZ ring that dictates the division site and the resultant polar morphology.

ACKNOWLEDGMENTS

This work was supported by grant GM29674 from the National Institutes of Health.

We thank Barbara Fegley for help with the scanning electron microscopy.

REFERENCES

1. **Bi, E., and J. Lutkenhaus.** 1990. FtsZ regulates frequency of cell division in *Escherichia coli*. J. Bacteriol. **172:**2765–2768.
2. **Bi, E., and J. Lutkenhaus.** 1990. Analysis of *ftsZ* mutations that confer resistance to the cell division inhibitor SulA (SfiA). J. Bacteriol. **172:**5602–5609.
3. **Bi, E., and J. Lutkenhaus.** 1990. Interaction between the *min* locus and *ftsZ*. J. Bacteriol. **172:**5610–5616.
4. **Bi, E., and J. Lutkenhaus.** 1991. FtsZ ring structure associated with cell division in *Escherichia coli*. Nature (London) **354:**161–164.
5. **Bukau, B., and G. C. Walker.** 1989. *ΔdnaK52* mutants of *Escherichia coli* have defects in chromosome segregation and plasmid maintenance at normal growth temperatures. J. Bacteriol. **171:**6030–6038.
6. **Dai, K., and J. Lutkenhaus.** 1991. *ftsZ* is an essential cell division gene in *Escherichia coli*. J. Bacteriol. **173:**3500–3506.
7. **Davis, R. W., D. Bothstein, and J. R. Roth.** 1980. Advanced bacterial genetics. Cold Spring Harbor Laboratory, Cold Spring Harbor, N.Y.
8. **de Boer, P. A. J., R. E. Crossley, and L. I. Rothfield.** 1989. A division inhibitor and a topological specificity factor coded for by the minicell locus determine proper placement of the division septum in *E. coli*. Cell **56:**641–649.
9. **Donachie, W. D., K. J. Begg, and N. F. Sullivan.** 1984. Morphogenes of *Escherichia coli*, p. 27–62. *In* R. Losick and L. Shapiro (ed.), Microbial development. Cold Spring Harbor Laboratory, Cold Spring Harbor, N.Y.
10. **Gottesman, S., E. Halpern, and P. Trisler.** 1981. Role of *sulA* and *sulB* in filamentation by *lon* mutants of *Escherichia coli* K-12. J. Bacteriol. **148:**265–273.
11. **Hiraga, S., H. Niki, T. Ogura, C. Ichinose, H. Mori, B. Exaki, and A. Jaffe.** 1989. Chromosome partitioning in *Escherichia coli*

novel mutants producing anucleate cells. J. Bacteriol. **171:**1496–1505.

12. **Huisman, O., R. D'Ari, and J. George.** 1980. Further characterization of *sfiA* and *sfiB* mutations in *Escherichia coli*. J. Bacteriol. **144:**185–191.
13. **Johnson, B. F.** 1977. Fine structure mapping and properties of mutations suppressing the *lon* mutation in *Escherichia coli* K12 and B strains. Genet. Res. **30:**273–286.
14. **Jones, C. A., and I. B. Holland.** 1985. Role of SfiB (FtsZ) protein in division inhibition during the SOS response in *Escherichia coli*. FtsZ stabilizes the inhibitor SfiA in maxicells. Proc. Natl. Acad. Sci. USA **82:**6045–6049.
15. **Lutkenhaus, J. F.** 1983. Coupling of DNA replication and cell division: *sulB* is an allele of *ftsZ*. J. Bacteriol. **154:**1339–1346.
16. **Lutkenhaus, J. F., H. Wolf-Watz, and W. D. Donachie.** 1980. Organization of genes in the *ftsA-envA* region of the *Escherichia coli* genetic map and identification of a new *fts* locus (*ftsZ*). J. Bacteriol. **142:**615–620.
17. **Miller, J. H.** 1972. Experiments in molecular genetics. Cold Spring Harbor Laboratory, Cold Spring Harbor, N.Y.
18. **Pla, J., M. Sanchez, P. Palacios, M. Vicente, and M. Aldea.** 1991. Preferential cytoplasmic location of FtsZ, a protein essential for *Escherichia coli* septation. Mol. Microbiol. **5:**1681–1686.
19. **Ripley, L. S.** 1990. Frameshift mutation: determinants of specificity. Annu. Rev. Genet. **24:**189–213.
20. **Spratt, B. G.** 1975. Distinct penicillin binding proteins involved in the division, elongation and shape of *Escherichia coli* K12. Proc. Natl. Acad. Sci. USA **72:**2999–3003.
21. **Taschner, P. E. M., N. Ypenburg, B. G. Spratt, and C. L. Woldringh.** 1988. An amino acid substitution in penicillin-binding protein 2 creates pointed polar caps in *Escherichia coli*. J. Bacteriol. **170:**4828–4837.
22. **Teather, R. M., J. F. Collins, and W. D. Donachie.** 1974. Quantal behavior of a diffusable factor which initiates septum formation at potential division sites in *Escherichia coli*. J. Bacteriol. **118:**407–413.
23. **Tormo, A., J. A. Ayala, M. A. DePedro, M. Aldea, and M. Vicente.** 1986. Interaction of FtsA and PBP3 proteins in the *Escherichia coli* septum. J. Bacteriol. **166:**985–992.
24. **Wang, X., P. A. J. de Boer, and L. I. Rothfield.** 1991. A factor that positively regulates cell division by activating transcription of the major cluster of essential cell division genes of *Escherichia coli*. EMBO J. **10:**3363–3372.
25. **Ward, J. E., Jr., and J. Lutkenhaus.** 1985. Overproduction of FtsZ induces minicell formation in *E. coli*. Cell **42:**941–949.